Induction of Pancreatic Differentiation by Signals from Blood Vessels

Eckhard Lammert,* Ondine Cleaver,* Douglas Melton†

Blood vessels supply developing organs with metabolic sustenance. Here, we demonstrate a role for blood vessels as a source of developmental signals during pancreatic organogenesis. In vitro experiments with embryonic mouse tissues demonstrate that blood vessel endothelium induces insulin expression in isolated endoderm. Removal of the dorsal aorta in *Xenopus laevis* embryos results in the failure of insulin expression in vivo. Furthermore, using transgenic mice, we show that ectopic vascularization in the posterior foregut leads to ectopic insulin expression and islet hyperplasia. These results indicate that vessels not only provide metabolic sustenance, but also provide inductive signals for organ development.

Vascular endothelium grows in coordination with all embryonic tissues and is essential for viability (*1, 2*). Its prevalence in the embryo is likely to be guided by vascular endothelial growth factor (VEGF). VEGF induces proliferation, migration, and differentiation of endothelial cells (*3*). The main receptors for VEGF—VEGFR1 and VEGFR2 (also known as Flk-1)—are expressed on endothelial cells and their precursors (*4*). Mice lacking a single VEGF allele die of severe vascular abnormalities (*5, 6*).

Here, we investigate the role of blood vessels during endocrine pancreatic development. Islets of Langerhans, composed of pancreatic endocrine cells, perform a vital metabolic role in vertebrates that depends on an intimate contact with blood vessels. Islets measure glucose levels in the blood and react by secreting endocrine hormones, predominantly insulin, into the circulatory system (*7*). In this report, we focus on endothelial induction of insulin gene expression, because insulin is expressed in differentiated endocrine cells and because of its critical role in insulin-dependent diabetes mellitus (IDDM). Unlike other pancreatic hormones, insulin expression is restricted to pancreatic tissue along the gastrointestinal tract.

Pancreatic growth is initiated at three sites in the foregut endoderm, precisely where the endodermal epithelium contacts the endothelium of major blood vessels (Fig. 1, A through F). At this stage, vessels are composed solely of endothelial cells and are not yet surrounded by smooth muscle or other supporting cells. At 9.0 days post coitus (dpc), the pancreatic rudiment is marked by expression of the homeobox gene *Pdx1* (*8, 9*) which is restricted to endoderm that contacts the endothelium of the vitelline veins and the fusing dorsal aortae (Fig. 1, E and F). Gut endoderm that is either anterior or posterior to the evaginating pancreatic buds is separated from the major blood vessels by mesenchyme at this stage (Fig. 1, A through D). Following endothelial contact, both dorsal and ventral *Pdx1* domains evaginate (Fig. 1G). At 10.5 dpc, insulin expression begins at sites where the dorsal pancreatic endoderm contacts portal vein endothelium (Fig. 1, H and I) (*10, 11*).

The interaction of blood vessels with endocrine cells continues when mature, hormone-secreting islets are formed after birth. As previously observed, islets express significant levels of VEGF (Fig. 1, J and K), specifically the VEGF120 and VEGF164 isoforms, and pancreatic endothelial cells express both VEGF receptors (*12*). VEGFR2-expressing capillaries surround not only islets but also pancreatic ducts, which may harbor islet precursors (Fig. 1, L through N) (*13*). Thus, pancreatic-endothelial interactions begin long before islets are functionally mature, and are maintained throughout islet formation, raising the issue of whether

Department of Molecular and Cellular Biology, Howard Hughes Medical Institute, Harvard University, 7 Divinity Avenue, Cambridge, MA 02138, USA.

*These authors contributed equally to this work.
†To whom correspondence should be addressed.

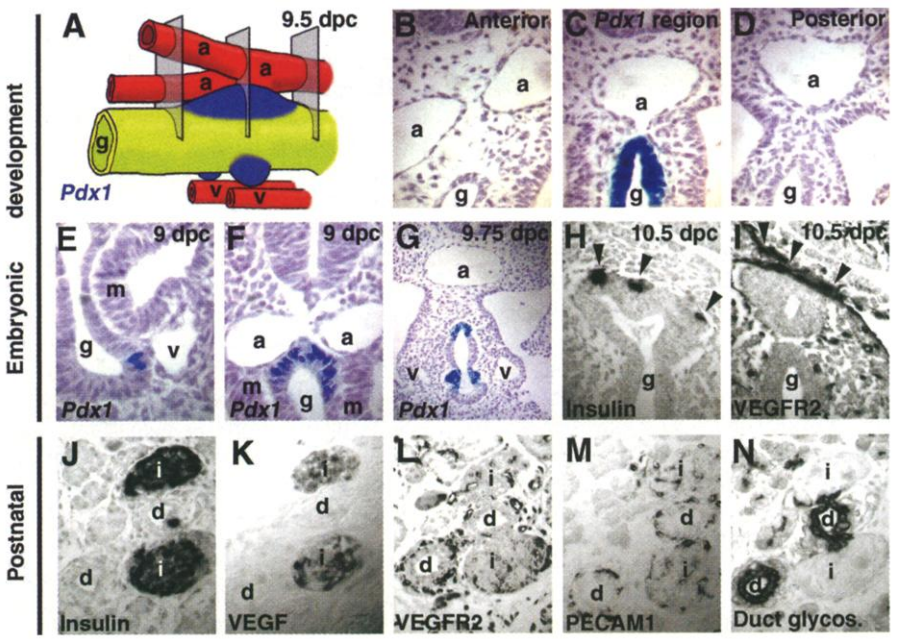

Fig. 1. Pancreatic budding and endocrine differentiation take place adjacent to blood vessels. (**A**) Schematic representation of blood vessels (red) relative to pancreatic endoderm expressing *Pdx1* (blue). The gut tube endoderm is yellow. Aortae (a), vitelline veins (v), and gut endoderm (g) are indicated. (B to D) Transverse sections through mouse foregut, as indicated in (A). Sections are taken from the same 9.5-dpc mouse embryo. (**B**) Section anterior to the *Pdx1* region. (**C**) Section through the *Pdx1* region. (**D**) Section posterior to the *Pdx1* region. (**E**) In the ventral gut tube (g) at 9 dpc, *Pdx1* expression begins in two ventral domains. One domain is shown here. *Pdx1* is initiated in the endoderm adjacent to the vitelline vein endothelium (v) and not in endoderm adjacent to mesenchyme (m). (**F**) *Pdx1* expression begins slightly later in the dorsal endoderm adjacent to the fusing dorsal aortae (a). (**G**) These *Pdx1*-expressing domains are budding from the gut tube at 9.75 dpc. (H and I) Adjacent transverse sections of the mouse gut tube at 10.5 dpc. Scattered cells expressing insulin develop in the dorsal pancreatic bud [arrowheads in (**H**)] adjacent to the right vitelline or portal vein as marked by VEGFR2 expression [sites of contact with insulin-expressing cells are marked with arrowheads in (**I**)]. (J through N) Adjacent sections of a neonatal p3 mouse pancreas are stained for insulin (**J**), VEGF (**K**), VEGFR2 (**L**), platelet endothelial-cell adhesion molecule 1 (PECAM1) (**M**), and duct glycosylation (**N**). Islets, i; ducts, d. Sections were stained as described (*28, 29*).

these tissues signal to each other during development.

To address signaling between tissues while excluding the effects of embryonic blood flow and metabolic exchange, endoderm and dorsal aortae were isolated from mouse embryos at 8.25 to 8.5 dpc and recombined in culture (Fig. 2 and Table 1) (*10*). At 8.5 dpc, midline endoderm is associated with the notochord and has not yet formed a tube (Fig. 2, A and B). The endoderm consists of tissue fated to become foregut and midgut, including the dorsal pancreas, but does not yet express pancreatic genes (*14*). The dorsal aortae lie immediately dorsal to the endoderm as two endothelial tubes, lateral to the notochord (Fig. 2, C and D) (*15*). Isolated endoderm, grown in culture for 6 days, formed a structure reminiscent of a gut tube, but did not exhibit signs of pancreatic differentiation, such as *Pdx1* or insulin expression (Fig. 2, E through H). In contrast, when isolated endoderm was cultured in combination with dorsal aortae, it initiated both *Pdx1* and insulin expression (Fig. 2, I through L, and Table 1). Approximately one-third of the recombinants formed structures resembling pancreatic buds (Fig. 2I). Insulin expression appeared adjacent to endothelium, as observed during normal development.

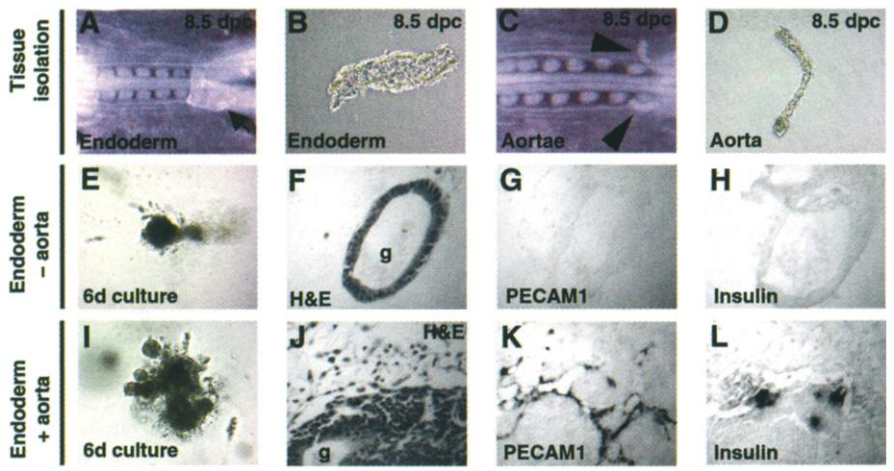

Fig. 2. Blood vessel endothelium induces insulin expression in isolated mouse endoderm. (**A** through **D**) Dorsal endoderm (arrow) and dorsal aortae (arrowheads) from the first to fifth somite region are isolated from mouse embryos at 8.25 to 8.5 dpc (8–10 somite stage). When cultured alone, the endoderm forms a gut tube–like structure (**E**), as shown by an H&E (hematoxylin/eosin)–stained section (**F**). No associated endothelial cells, as assayed by PECAM1 expression (**G**), and no endocrine cells, as assayed by insulin expression (**H**), are detected on adjacent sections. (I through L) When the endoderm is recombined with aorta endothelium (**I**), it forms a tube-like structure as seen by H&E staining (**J**), exhibits budding (I), and expresses insulin (**L**) adjacent to aorta endothelium (**K**).

Recombination of prepancreatic endoderm with other tissues harboring endothelial cells, including the lateral plate mesenchyme and umbilical artery, also lead to pancreatic differentiation (Table 1) (*10*). In contrast, tissues such as the notochord or neural tube did not induce insulin expression in isolated endoderm. The notochord induced *Pdx1*, but never insulin, in these mouse endodermal explants (Table 1). Our previous work with chick embryos showed that the notochord induced both *Pdx1* and insulin [(*16*); for discussion, see (*17*)]. To demonstrate that the isolated aortae did not carry along residual insulin cell precursors, we recombined dorsal aortae with other tissues such as somites and neural tube, and yet insulin expression was never observed in these recombinants (Table 1). These results indicate that insulin expression is induced in competent prepancreatic endoderm and that endothelium supplies signals sufficient for insulin expression.

To assess the requirement for endothelial signals during endocrine cell differentiation in vivo, we generated *Xenopus* embryos lacking a dorsal aorta (*18*) and examined the consequences on pancreatic development (*19*). The expression of insulin and two endocrine transcription factors, *NeuroD* (*20*) and *Pax6* (*21*), marks the dorsal pancreatic anlage in *Xenopus* (*22*). Embryos lacking a dorsal aorta displayed a strong reduction or elimination of insulin, *NeuroD*, and *Pax6* expression in all dissected embryos (Fig. 3, A through F) (*10*). These results indicate that endothelial signals are required for endocrine cell differentiation in frog embryos.

Blocking aorta formation is accomplished by excising intermediate mesoderm, which contains aortic precursors (*18*). Controls demonstrated that the dissection procedure did not adversely affect tissues located nearby, including the notochord, hypochord, gut tube, and floor plate. This was shown by normal notochord development (Fig. 3, G and J), the normal expression patterns for *F-spondin* (*23*) in the hypochord and floor plate (Fig. 3, H and K), and *XHex* expression (*24*) in liver and thyroid endoderm (Fig. 3, I and L). We note that *Xenopus* embryos did not express endocrine pancreatic genes, despite the presence of the notochord, when aorta formation was prevented. Moreover, the absence of the intermediate mesoderm by itself did not result in failure of

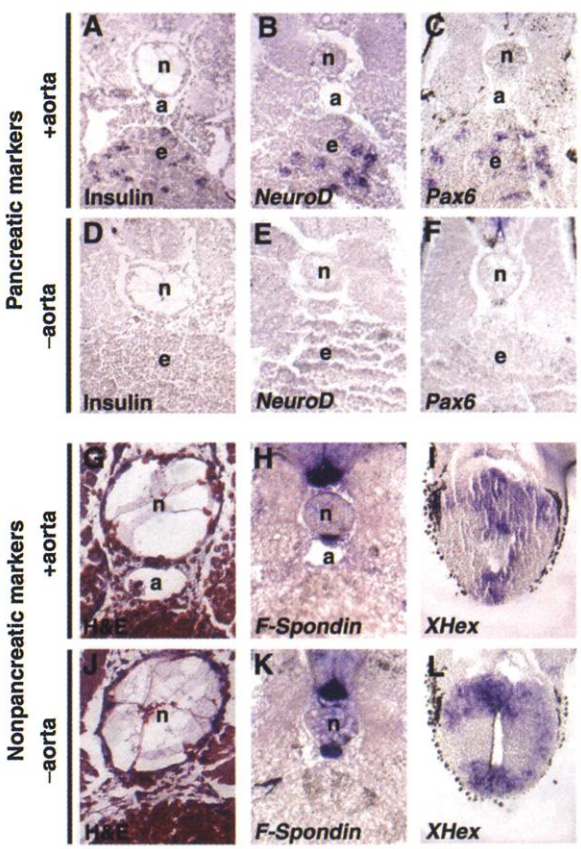

Fig. 3. (**A** through **F**) The dorsal aorta is necessary for endocrine pancreatic differentiation in stage 39–40 *Xenopus* embryos. Immunohistochemistry for insulin and in situ hybridization for *NeuroD* and *Pax6* in the pancreatic anlage of unmanipulated embryos (A to C) and dissected embryos (D to F). (**G** through **L**) In situ hybridization for *F-spondin* in the floor plate and hypochord, and *XHex* in the liver, indicates that midline development of mesoderm and endoderm can proceed normally in the absence of the dorsal aorta, subsequent to the dissection procedure. Notochord (n), aorta (a), and endoderm (e) are indicated. (G and J) H&E-stained sections show the absence of the dorsal aorta in dissected embryos.

endocrine development, because embryos lacking intermediate mesoderm expressed insulin when endothelium was present (*10*). Thus, endocrine pancreatic gene expression in *Xenopus* invariably correlates with the presence of endothelial tissue.

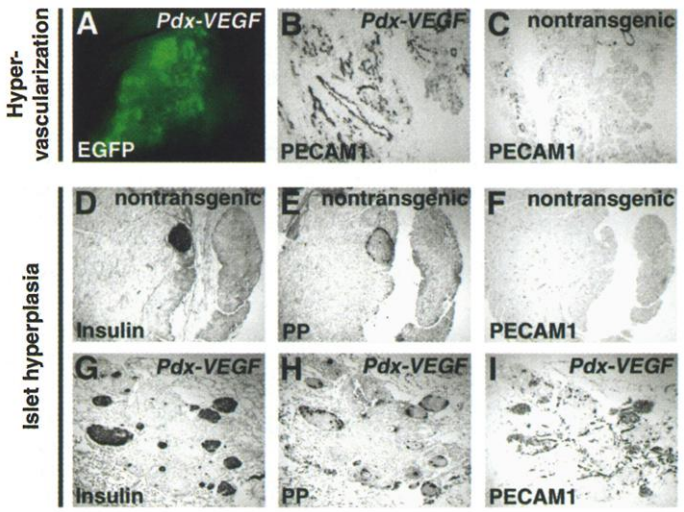

Fig. 4. Hypervascularization of the pancreas results in islet hyperplasia. (**A**) Expression of the *Pdx-VEGF* transgene in 15.5-dpc embryonic pancreas is assayed by EGFP fluorescence in the pancreas. (**B**) Transgenic embryos display hypervascularization of pancreatic tissue, as assayed by PECAM1 when compared with (**C**) nontransgenic controls. (**D** through **I**) Islet hyperplasia in the pancreas of transgenic animals at 2 months. Adjacent pancreas sections from *Pdx-VEGF* transgenic mice (G through I) are compared with nontransgenic littermates (D through F). Sections are stained for insulin (D and G), pancreatic polypeptide PP (E and H), and PECAM1 (F and I).

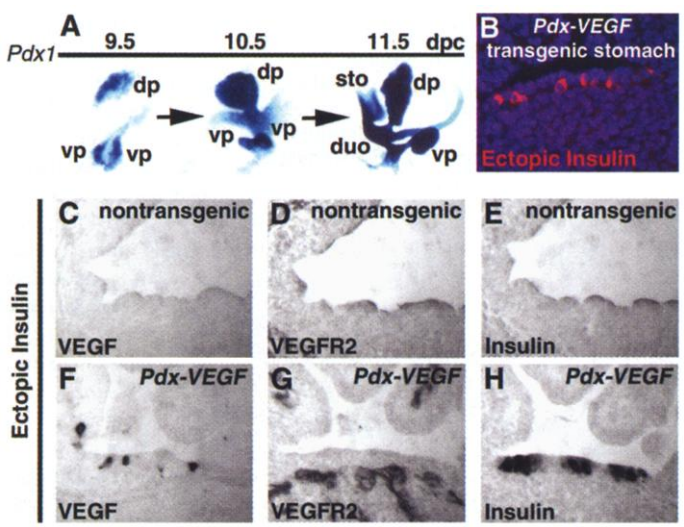

Fig. 5. Ectopic vascularization leads to ectopic insulin expression. (**A**) *Pdx1* expression as detected by a lacZ gene inserted into the *Pdx1* locus (*9*). Cleared embryos at 9.5, 10.5, and 11.5 dpc show that *Pdx1* expression expands beyond the dorsal (dp) and ventral (vp) pancreatic buds, to the duodenum (duo) and stomach (sto) during embryonic development. (**B**) Staining for insulin (red) and DAPI nuclei (blue) staining on a 5-μm stomach section of a 15.5-dpc *Pdx-VEGF* transgenic mouse. Adjacent stomach sections of transgenic mice (**F** through **H**) are compared with nontransgenic littermates (**C** through **E**). Sections are stained for VEGF (C and F), VEGFR2 (D and G), and insulin (E and H).

Table 1. In vitro recombination of 8.25- to 8.5-dpc mouse tissues demonstrates that endothelial signals induce pancreatic differentiation in isolated endoderm. Tissues used for *Pdx1* analysis are taken from progeny of matings of mice heterozygous for a lacZ insertion into the *Pdx1* locus with ICR mice (half should contain the insertion). Ratios of explants expressing insulin (as determined by antibody staining) and *Pdx1* (as determined by LacZ staining) versus total number of explants are shown. n.d., not done.

Recombined tissues	Insulin-expressing explants/total number of explants	*Pdx1*-expressing explants/total number of explants
Endoderm + aorta	7/10	17/36
Endoderm	0/5	0/8
Endoderm + umbilical artery	3/6	4/8
Endoderm + mesenchyme	3/6	3/6
Endoderm + notochord	0/6	4/16
Endoderm + neural tube	0/7	0/1
Aorta + neural tube	0/3	n.d.
Aorta + somites	0/4	n.d.

To assay blood vessel–pancreas interactions later in development, we constructed a mouse transgene in which *VEGF164*, coexpressed with *EGFP* (enhanced green fluorescent protein), is driven by the *Pdx1* promoter (*10, 25*). During murine embryogenesis, *Pdx1* is expressed throughout the pancreas and parts of the stomach and duodenum (see below), and becomes progressively restricted to islets by birth (*9, 26*). Animals with strong VEGF expression could therefore be selected by the presence of green fluorescence in the dorsal pancreas (Fig. 4A). As a result of VEGF expression (*10*), fluorescent *Pdx-VEGF* transgenic animals displayed a marked increase in vascular endothelium (compare Fig. 4B with 4C).

At 2 months of age, *Pdx-VEGF* transgenic mice had a cystic, hypervascularized pancreas and islet hyperplasia (compare Fig. 4, D through F, and Fig. 4, G through I). *Pdx-VEGF* transgenic mice displayed a threefold increase in islet number and islet area, accompanied by a sevenfold decrease in the acini area (*10, 27*). Evidently, endocrine cell types were promoted at the expense of acinar cell types. Transgenic islets revealed a normal islet morphology (Fig. 4, G and H) (*10*).

Previous work (*8, 9*) had shown that after its initial localization in pancreatic buds at 9.5 dpc, *Pdx1* expression expands to the posterior part of the stomach and to the duodenum by 11.5 dpc (Fig. 5A). We therefore examined the stomach and duodenum of *Pdx-VEGF* transgenic embryos for developmental effects in transient transgenic experiments. At 15.5 dpc, five of five transgenic embryos with strong fluorescence had ectopic insulin-expressing cells in the posterior stomach epithelium (Fig. 5, B and H). Insulin expression was not detected in the stomach of nontransgenic littermates (0 of 20, Fig. 5E). A comparison of transgenic and nontransgenic littermates demonstrated that ectopic insulin-expressing cells were found directly adjacent to ectopically induced endothelial cells (compare Fig. 5, D and E, with Fig. 5, G and H). These cells were located within the *Pdx1*-expressing posterior stomach epithelium. Insulin-expressing cells were found neither in the hypervascularized stomach mesenchyme nor in the epithelium outside the *Pdx1* region (Fig. 5, B and H). Thus, it is likely that the ectopic insulin-positive cells developed from *Pdx1*-expressing precursor cells within the stomach epithelium. The degree of ectopic insulin expression in the epithelium correlated directly with the degree of hypervascularization (*10*). In two of five transgenic animals, an ectopic budlike structure was observed in the anterior duodenum (*10*). The ectopic bud had particularly high levels of *VEGF* transgene expression and scattered insulin-expressing cells.

In this study, we have used three different experimental systems to demonstrate a role for blood vessels as a source for developmental signals during pancreatic organogenesis. Specif-

ically, we showed that blood vessel endothelium induces endocrine pancreatic differentiation. Taken together with previous embryological work (*14, 16*), these data indicate that prepancreatic endoderm is patterned in a stepwise manner, beginning with signals from the mesoderm/ectoderm at 7.5 dpc (*14*), followed by signals from the notochord during the next day (*16*). The blood vessel endothelium then provides the prepatterned endoderm with additional signals that induce differentiation of insulin-expressing cells. The fact that early endoderm, including the prepancreatic region, expresses VEGF (*4*) could explain how the vessels are attracted to the growing pancreas and islets. In a broader context, our data suggest that the close physiological relationship between blood vessels and islets in the pancreas depends on inductive interactions that begin at the earliest stages of development. This type of mutual signaling between tissues and blood vessels during development may be a general mechanism used in vertebrate organogenesis.

References and Notes

1. G. H. Fong, J. Rossant, M. Gertsenstein, M. L. Breitman, *Nature* **376**, 66 (1995).
2. F. Shalaby *et al.*, *Nature* **376**, 62 (1995).
3. N. Ferrara, *J. Mol. Med.* **77**, 527 (1999).
4. D. J. Dumont *et al.*, *Dev. Dyn.* **203**, 80 (1995).
5. P. Carmeliet *et al.*, *Nature* **380**, 435 (1996).
6. N. Ferrara *et al.*, *Nature* **380**, 439 (1996).
7. F. G. Banting, C. H. Best, *J. Lab. Clin. Med.* **115**, 254 (1990).
8. J. Jonsson, L. Carlsson, T. Edlund, H. Edlund, *Nature* **371**, 606 (1994).
9. M. F. Offield *et al.*, *Development* **122**, 983 (1996).
10. Supplementary Web material is available at *Science* Online at www.sciencemag.org/cgi/content/full/1064344/DC1
11. Mouse pancreatic development is initially symmetric (Fig. 1, A through G, and Fig. 5A) with three buds forming adjacent to the dorsal aorta and the two vitelline veins. This is also seen in frog embryos, where the dorsal bud contacts the dorsal aorta, and each ventral bud is adjacent to a vitelline vein plexus (*22*). In mice, we observed that only one of the two ventral pancreatic buds develops into pancreatic tissue, whereas the other bud regresses, coinciding with a developing asymmetry of vitelline veins. The ventral bud adjacent to the endothelium of the right vitelline (portal) vein continues to grow and develop, whereas the left ventral bud disappears together with the left vitelline vein.
12. G. Christofori, P. Naik, D. Hanahan, *Mol. Endocrinol.* **9**, 1760 (1995).
13. G. Teitelman, J. Lee, D. J. Reis, *Dev. Biol.* **120**, 425 (1987).
14. J. M. Wells, D. A. Melton, *Development* **127**, 1563 (2000).
15. Aortic endothelium is removed at 8.25 to 8.5 dpc, a stage when endothelial cells have just recently coalesced into tubes and when supporting mural cells have not yet started to envelop the endothelium of the blood vessels. To ensure isolation of purified endothelium, we used enzymatic treatment to remove any adhering mesenchymal cells (*10*).
16. S. K. Kim, M. Hebrok, D. A. Melton, *Development* **124**, 4243 (1997).
17. There are two possible explanations for the difference in insulin expression induced by the notochord in chick and mouse endodermal explants. There may be a fundamental mechanistic difference between chick and mouse. However, we favor the possibility that chick endodermal explants may have contained contaminating endothelial cells. Endothelial tissues are pervasive and difficult to detect at early stages of chick development. Without enzymatic treatment to eliminate adhering endothelium or specific assays to detect endothelial cells, it is difficult to rule out contamination.
18. O. Cleaver, P. A. Krieg, *Development* **125**, 3905 (1998).
19. During the removal of the intermediate mesoderm, damage to the underlying endoderm results in immediate extrusion of yolky cellular material from the large endodermal cells. Any embryo incurring such damage was identifiable and immediately discarded (*10*).
20. J. E. Lee *et al.*, *Science* **268**, 836 (1995).
21. N. Hirsch, W. A. Harris, *J. Neurobiol.* **32**, 45 (1997).
22. O. G. Kelly, D. A. Melton, *Dev. Dyn.* **218**, 615 (2000).
23. A. Ruiz, I. Altaba, C. Cox, T. M. Jessel, A. Klar, *Proc. Natl. Acad. Sci. U.S.A.* **90**, 8268 (1993).
24. C. S. Newman, F. Chia, P. A. Krieg, *Mech. Dev.* **66**, 83 (1997).
25. A total of 11 fluorescent *Pdx-VEGF* animals derived from independent microinjections were analyzed (five at 15.5 dpc, five at birth, and one stable line). Five of five fluorescent neonates displayed a hyperplastic distribution of islets at birth. To rule out nonspecific effects of *Pdx1*-driven EGFP, a transgene driving only *IRES-EGFP* under the *Pdx1* promoter was used. Three of three fluorescent *Pdx-EGFP* transgenic mice had a normal distribution of insulin expressing islets and amylase expressing acini.
26. K. L. Wu *et al.*, *Mol. Cell. Biol.* **17**, 6002 (1997).
27. It is likely that islet hyperplasia in transgenics is caused by an increased number of blood vessels rather than a direct effect of VEGF on pancreatic epithelium. Two different anti-VEGFR2 antibodies stain blood vessels, but not pancreatic epithelial cells, suggesting that the latter tissue cannot respond directly to VEGF. Our results agree with a study showing VEGF receptor expression in capillary endothelium within the pancreas (*12*).
28. E. Lammert, J. Brown, D. A. Melton, *Mech. Dev.* **94**, 199 (2000).
29. R. A. Brekken, X. Huang, S. W. King, P. E. Thorpe, *Cancer Res.* **58**, 1952 (1998).

30. We thank J. Dubauskaite for the production of transgenic mice. We are grateful to R. Brekken, C. V. Wright, A. Nagy, and P. A. Krieg for essential reagents (*10*). We also thank A. P. McMahon, P. A. Krieg, Y. Dor, J. Wells, A. Grapin-Botton, L. Murtaugh, and T. Carroll for critical comments. E.L. was supported by the Deutsche Forschungsgemeinschaft (La 1216/1-1) and is currently supported by the American Diabetes Association, O.C. is supported by the Cancer Research Fund of the Damon Runyon–Walter Winchell Foundation Fellowship (DRG 1534), and D.M. is an investigator of the Howard Hughes Medical Institute.

12 July 2000; accepted 12 September 2001
Published online 27 September 2001;
10.1126/science.1064344
Include this information when citing this paper.

Charge Migration in DNA: Ion-Gated Transport

Robert N. Barnett,[1] Charles L. Cleveland,[1] Abraham Joy,[2] Uzi Landman,[1]* Gary B. Schuster[2]*

Electron hole (radical cation) migration in DNA, where the quantum transport of an injected charge is gated in a correlated manner by the thermal motions of the hydrated counterions, is described here. Classical molecular dynamics simulations in conjunction with large-scale first-principles electronic structure calculations reveal that different counterion configurations lead to formation of states characterized by varying spatial distributions and degrees of charge localization. Stochastic dynamic fluctuations between such ionic configurations can induce correlated changes in the spatial distribution of the hole, with concomitant transport along the DNA double helix. Comparative ultraviolet light–induced cleavage experiments on native B DNA oligomers and on ones modified to contain counterion (Na^+)-starved bridges between damage-susceptible hole-trapping sites called GG steps show in the latter a reduction in damage at the distal step. This reduction indicates a reduced mobility of the hole across the modified bridge as predicted theoretically.

Recent experiments have established that hole (radical cation) transport occurs in DNA to distant sites (*1–4*), and these results have led to speculation that trapping sites evolved to protect genomic DNA from oxidative reactions (*5*). Long-range charge transport in DNA is being assessed for application to nanoelectronic technologies (*6*), and intensive research has been aimed at elucidation of the energetics and dynamics of charge migration in DNA (*7*) both in vivo, (*8*, *9*) and in solution (*1–4*, *10*).

Exploration of charge transport in DNA has focused on studies of synthetic oligomers labeled with redox probes that are initiated by photochemical or electrochemical techniques and assessed by spectroscopic or chemical methods (*1–4*, *11*). These efforts were designed to elucidate the factors that control the elementary steps of charge injection, transport, and trapping to test their dependencies on base-sequence, in particular, and to test theoretical models centered on phenomenological kinetic schemes (*12–14*). Transport models include (i) A coherent single-step tun-

[1]School of Physics, [2]School of Chemistry and Biochemistry, Georgia Institute of Technology, Atlanta, GA 30332, USA.

*To whom correspondence should be addressed. E-mail: uzi.landman@physics.gatech.edu (U.L.); gary.schuster@cos.gatech.edu (G.B.S.)